Colloid and Interface Science Communications 40 (2021) 100343

Contents lists available at ScienceDirect

Colloid and Interface Science Communications

journal homepage: www.elsevier.com/locate/colcom

Rapid Communication

Reactive wetting of polyethylene on ethylene-propylene-diene terpolymer

Brittany Laing [a,*], David Seveno [b], Jozefien De Keyzer [c], Albert Van Bael [a,b]

[a] KU Leuven, Department of Materials Engineering, Diepenbeek Campus, Wetenschapspark 27, 3590 Diepenbeek, Belgium
[b] KU Leuven, Department of Materials Engineering, Leuven Campus, Kasteelpark Arenberg 44, 3001 Leuven, Belgium
[c] KU Leuven, Department of Chemical Engineering, Diepenbeek Campus, Wetenschapspark 27, 3590 Diepenbeek, Belgium

ARTICLE INFO

Keywords:
Reactive wetting
Ethylene-propylene-diene terpolymer
Polyethylene
Vulcanization
Adhesion

ABSTRACT

If wetting is ubiquitous in nature, reactive wetting is up to now mostly described for metallic and ceramic systems. Characterizing wetting between two reactive organic polymers is more challenging due to their similar molecular structure and yet it is crucial to unravel adhesion mechanisms. This is for example the case when combining ethylene-propylene-diene terpolymer (EPDM) with polyolefins like polyethylene (PE). Therefore, in this study, a high temperature contact angle measurement methodology is presented to evidence the occurrence of chemical bonds at the interface. Spreading of PE was found to be restricted on vulcanizing peroxide-based EPDM, while on an already completely vulcanized EPDM, low static advancing contact angles were obtained. This restriction in wetting is ascribed to a co-vulcanization reaction between EPDM and PE. Furthermore, the chemical bonding mechanism is even more pronounced with higher peroxide concentrations in EPDM which also leads to a higher adhesion strength at the interface.

1. Introduction

Adhesion between two polymer surfaces is a complex phenomenon related to intermolecular interactions. Depending on the specific material composition, dispersive interactions, acid-base interactions, interdiffusion (leading to intermingling or/and entanglement), and/or chemical bonding can be created [1,2]. Regardless of the adhesion mechanisms, intimate contacts between the two polymer surfaces is a prerequisite, i.e. wetting must be ensured [3]. When a liquid wets a solid substrate, spreading usually occurs through a physical process leading to an increase of the liquid coverage area in time after droplet deposition [4]. This process is referred to as non-reactive wetting as no reaction between the liquid and substrates occurs. Contact angle analysis during wetting has been extensively studied and reviewed in literature with regards to static and dynamic spreading, solid surface tension and surface heterogeneities [4–9]. Specifically for wetting of molten polymers, studies have been done on glass substrates, bulk metallic glasses, tool steel surfaces, coatings and vulcanized rubbers by direct contact angle measurements to understand wetting behavior close-to-processing conditions [10–14]. When topographic heterogeneity applies, it is important that the molten polymer is able to fully wet the rough surface as this increases contact area promoting further physical or chemical adhesion mechanisms [4,13,15]. During contact angle measurements, chemical reactions between the liquid and solid substrate can also alter the solid/liquid interface and consequently the wetting process [4,16]. Reactive wetting is well reported in metal-metal joining processes like brazing and soldering, or in metal-ceramic processes [17–19]. In contrast, reactive wetting triggered by a polymer melt is limited in literature. In studies by Grundke et al. [1,20], the wetting kinetics of unmodified and chemically modified polypropylene melts on untreated and aminosilane-treated glass fibers were characterized, evidencing the role of physical or chemical interactions at the interface [20]. Furthermore, an interfacial chemical reaction was created between a maleic anhydride copolymer melt and poly(aminosiloxane) surface during wetting which acted as an additional driving force for the spreading process [1]. Similarly, Fuentes et al. [13] observed a reduction in static contact angles with increasing maleic anhydride (MA) content in molten maleic anhydride-grafted polypropylene (MAPP)/polypropylene (PP) blends which was explained by covalent bonding between the MA groups and the glass substrate. For the combination of a thermoset rubber solid and thermoplastic melt, literature on reactive wetting is currently, to the best of our knowledge, lacking despite its importance for two-component (2K) injection molding of thermoset rubber with thermoplastics [21–23].

During the injection of a 2K rubber/thermoplastic composite, a thermoplastic molten zone is created near the rubber/thermoplastic

* Corresponding author.
E-mail address: brittany.laing@kuleuven.be (B. Laing).

https://doi.org/10.1016/j.colcom.2020.100343
Received 8 September 2020; Received in revised form 9 November 2020; Accepted 15 November 2020
Available online 6 December 2020

interface, while vulcanization occurs in the rubber part [21,23]. Consequently, adhesion mechanisms like chemical bonding and/or interdiffusion may be initiated. The occurrence of these mechanisms depends on the specific curing system, i.e. sulfur or peroxide curing, applied in the rubber. Laing et al. [24,25] already studied this phenomenon in previous studies focusing on the influences of the curing agent and co-agents in a peroxide curing system. In contrast to sulfur curing, peroxide curing may cause co-vulcanization between ethylene-propylene-diene terpolymer (EPDM) and polyethylene (PE) at the interface as no unsaturations are required for crosslinking. However, a clear characterization of the adhesion mechanism at the interface is currently lacking. Typical techniques to evaluate chemical bonding are X-Ray Photoelectron Spectroscopy (XPS), Time-of-Flight Secondary Ion Mass Spectroscopy (ToF-SIMS), Attenuated Total Reflectance Fourier Transform Infrared Spectroscopy (ATR-FTIR) and confocal Raman spectroscopy as they can identify chemical groups at a substrate surface [13,26,27]. Specifically at the interface between EPDM and PE, a co-vulcanization reaction might lead to allyl/alkyl, alkyl/alkyl and alkene/alkyl crosslinks which are all composed of carbon-carbon (C—C) bonds [25]. As indicated by Orza et al. [28] these crosslinks are also present in EPDM, so that these techniques cannot distinguish the C-C/C-H in PE from these of EPDM and the interfacial crosslinks as both polymers contain aliphatic carbons. Therefore, an attempt was made to use contact angle measurements to characterize chemical bonding between a polymer melt and an EPDM substrate due to reactive wetting [1,4]. Specifically, reactive wetting, i.e. simultaneous spreading and formation of covalent bonds, of a thermoplastic melt on initially unvulcanized peroxide-based EPDM is studied both from wetting and practical adhesion aspects. Wetting on peroxide-based EPDM is also compared to wetting on sulfur-based EPDM, and the influence of peroxide curing agent concentration is analyzed as this can cause reactivity differences near the interface.

2. Experimental

All EPDM compounds were mixed and supplied by Hercorub NV. A peroxide-based EPDM compound was selected with dicumylperoxide (DCP) as curing agent. As a higher DCP concentration may cause more interfacial crosslinks [25], a comparison was made between 2 phr and 8 phr (parts per hundred parts of rubber) DCP with respective sample names DCP2 and DCP8. Additionally, a third compound was selected, S1, which is sulfur-based EPDM to analyze differences in spreading with peroxide-based EPDM. A detailed description of the formulations of EPDM compounds DCP2, DCP8 and S1 is given in Appendix A supplementary data (Table S1). As thermoplastic material, a high-density polyethylene (PE) grade M80064 (Sabic) (melting temperature = 135 °C, yield stress = 32 MPa) was selected to evaluate the adhesion with EPDM.

To measure the adhesion strength between the two polymers, 2K injection molded samples were produced in a versatile mold with a thermoplastic and a rubber cavity on an Engel ES330H/80 V/80HL-F equipped with a vertical rubber unit and a horizontal thermoplastic injection unit according the process developed by Bex et al. [21,23]. First, the thermoplastic parts were injection molded separately (40 × 150 × 2 mm) in the thermoplastic cavity, while a metal insert was placed in the rubber cavity. Afterwards, this metal insert was removed, the thermoplastic part was placed in the 2K mold and overmolded with EPDM, resulting in 2K specimens with dimensions 80 × 150 × 2 mm (Fig. S1). The specific injection molding parameters for the individual components are listed in Table S2. During the overmolding step with EPDM, the rubber cavity was set at a high temperature (180 °C) to cure the rubber, while the thermoplastic cavity was set at a low temperature (80 °C). Consequently, an intermediate temperature is reached at the interface around the melting point of the thermoplastic, creating a narrow melted thermoplastic zone at the interface and enabling adhesion with EPDM. Adhesion strength was evaluated by tensile testing. A detailed description of the 2K samples preparation and adhesion strength evaluation can be found in previous work by the authors [25]. Unvulcanized EPDM samples were produced as well for the contact angle measurements. These were injected in the rubber cavity with the EPDM injection molding parameters (Table S2). However, the mold cavities were set at 80 °C to prevent vulcanization. Consequently, both vulcanized and unvulcanized EPDM substrates had similar sample dimensions. The average roughness values (Ra) of the vulcanized rubber substrates, based on a three measurements with a Diavite Compact VHF (measuring length = 4.8 mm; cutoff = 0.8 mm), were 0.47 ± 0.09 μm for DCP2, 0.49 ± 0.10 μm for DCP8 and 0.46 ± 0.21 μm for S1; for the unvulcanized rubber substrates the Ra values were 0.66 ± 0.22 μm for DCP2, 0.83 ± 0.31 μm for DCP8 and 2.05 ± 0.39 μm for S1. The roughness measurements were executed before starting the wetting experiments.

For the wetting experiments, a high temperature contact angle measurement device from Dataphysics OCA 15 plus was used. In Fig. S2, the experimental setup of this device is schematically represented. The electrical heating within the chamber is controlled by a Dataphysics TEC 350 temperature control unit which enables a chamber temperature between 40 °C and 350 °C. The temperature within chamber, right above the PE granule, was measured and controlled with a thermocouple. During measurement, the temperature (T_H) above the granule had a maximum deviation of $T_H \pm 2$ °C. Measurements were carried out under an inert atmosphere (Nitrogen gas ≥99.999%, ALPHAGAZ™ 1, Air Liquide) to prevent oxidative degradation of the polymers. A CCD camera was used with a resolution of 768 × 576 pixels and a frame rate of 30 frames per seconds. Furthermore, contact angles between the PE melt and EPDM substrate were calculated with Dataphysics SCA 202 analysis software. Before starting the measurements, the heated chamber was stabilized under nitrogen flow for 5 min. The surface of the EPDM substrate was cleaned carefully with isopropanol (99.5%, Sigma-Aldrich) using a tissue. This cleaning step did not change substrates' surface roughness.

First, the vulcanization process of the unvulcanized EPDM substrates (DCP2, DCP8 and S1) was evaluated directly in the heated chamber. Indeed, without applying pressure, bubbles may form at the surface due to released gasses, resulting from the curing decomposition products [29], and modify the topography of the surface. It is however important to select a suitable temperature which preserves a smooth substrate surface. Unvulcanized EPDM substrates (10 × 10 × 2 mm) were then exposed to 140 °C, 150 °C, 160 °C and 170 °C. At each temperature, samples were evaluated after 5, 10, 15, 20, 25 and 30 min to analyze the substrate surface (Keyence VHX-500F digital microscope). Furthermore, vulcanization needed to be ensured at the selected temperature. Therefore, vulcanization degree after 30 min was assessed by Shore A hardness measurements (CV Shore A hardness durometer) [24] and an additional verification of the vulcanization behavior was executed with a moving die rheometer (MDR2000E, Monsanto).

Then, the wetting behaviors of PE on vulcanized and unvulcanized DCP2, DCP8 and S1 were compared. The vulcanized EPDM substrates were taken from EPDM bulk vulcanized at 180 °C, ensuring complete vulcanization. The EPDM substrate (10 × 10 × 2 mm) was placed in the heated chamber and immediately afterwards, the PE granule was placed on top of it with the spherical side facing down (average PE weight at T = 25 °C: 11.6 ± 0.7 mg), see Fig. S2. Consequently, the interaction between the melting/molten PE on vulcanizing EPDM from the initial start of curing could be evaluated. Contact angles were registered every minute during 30 min. The evolution from solid to molten stage lasted 3 min. From then on, contact angles could be calculated through an ellipse fitting. Fig. S3 shows a fitting of a PE droplet on vulcanized and unvulcanized DCP8 after 5 min and after 30 min. Three measurements were performed for each combination of PE with EPDM and average values with their 95% confidence intervals are reported.

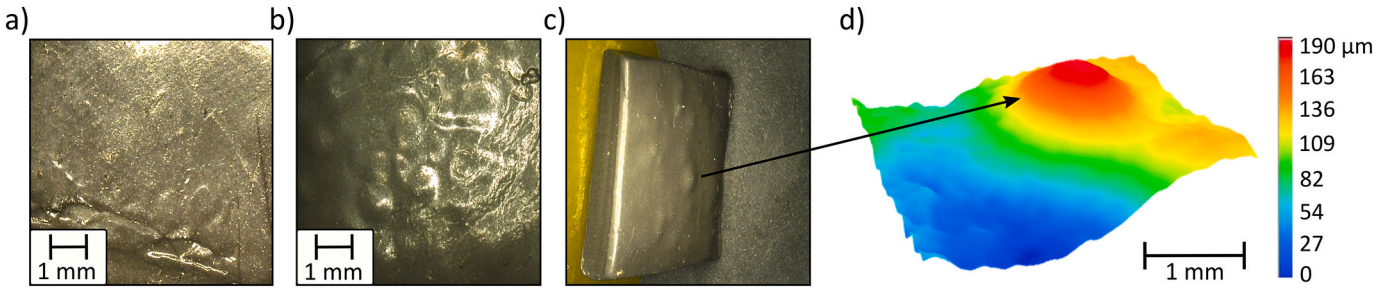

Fig. 1. Microscopic images of DCP2 substrate surface after 30 min at (a) 150 °C, (b) 160 °C and of DCP 8 at (c) 160 °C. In (c) the image represents a side view of the complete DCP8 substrate (10 × 10 × 2 mm) to illustrate the surface topography. (d) 3D image of a gas bubble from the DCP8 substrate.

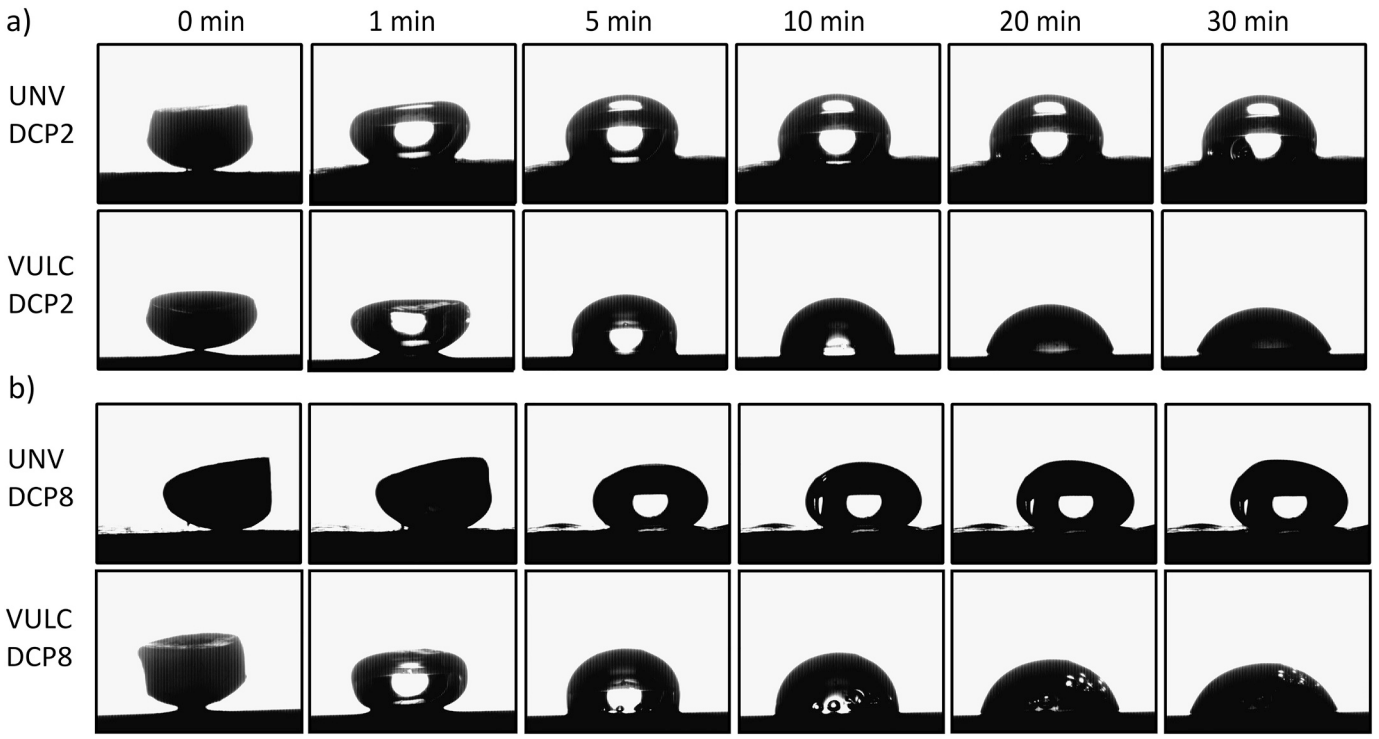

Fig. 2. Spreading of PE granule on (a) DCP2 and (b) DCP8 at 150 °C. At 0 min the PE granule is in solid state. 'UNV' refers to unvulcanized and 'VULC' refers to vulcanized.

3. Results and discussion

First, it was necessary to identify the best trade-off temperature that ensures a stable substrate surface (no gas bubbles), vulcanization of initially unvulcanized EPDM, and melting of PE. At 140 °C, no bubbles occurred at the substrates' surfaces after 30 min. At 150 °C, formation of bubbles still remained insignificant during 30 min (Fig. 1a). However, at 160 °C and 170 °C gas bubbles started to appear even after 5 min

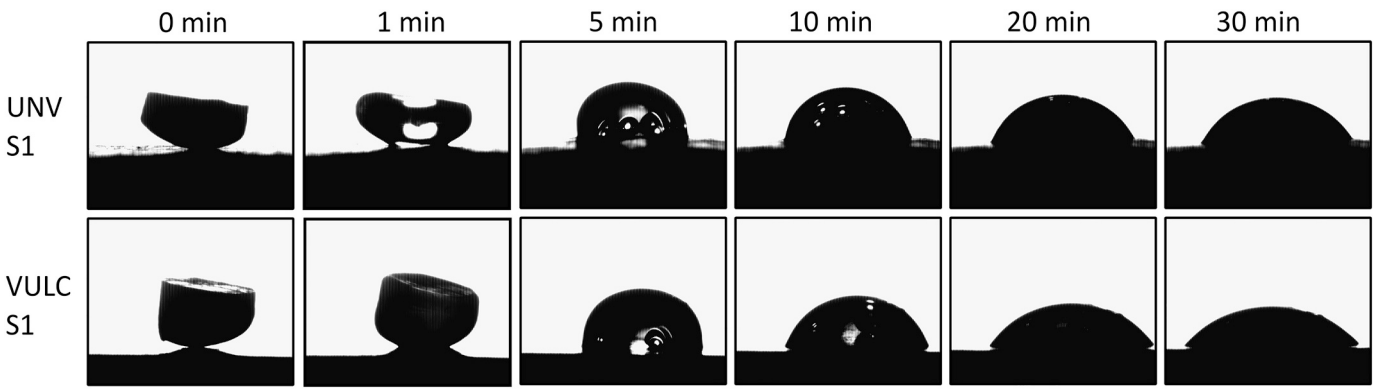

Fig. 3. Spreading of PE granule on S1 at 150 °C. At 0 min the PE granule is in solid state. 'UNV' refers to unvulcanized and 'VULC' refers to vulcanized.

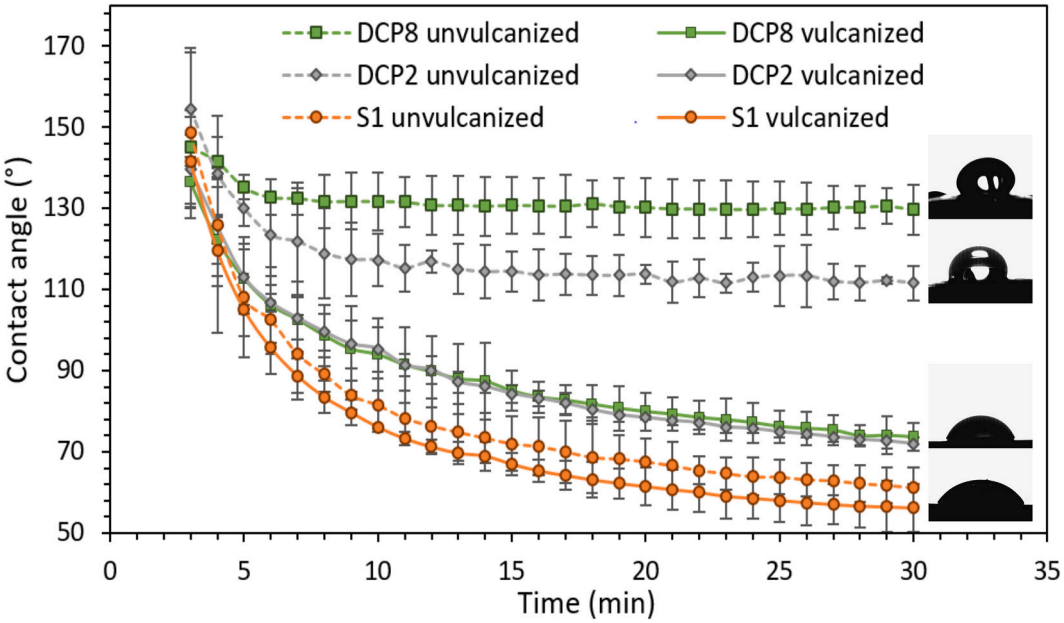

Fig. 4. Contact angle measurements of PE melt (150 °C) on DCP2, DCP8 and S1. Error bars represent 95% confidence interval.

inducing a change of the surface topography as illustrated by Fig. 1b and c. Fig. 1d represents a 3D view of one of the largest detected bubbles (height of 190 μm). On DCP2 small bubbles appeared on the complete sample surface while S1 and DCP8 had less but larger bubbles at 160 °C. This change in topography will influence the dynamic process of spreading of the thermoplastic melt during contact angle measurements. Therefore, a measuring temperature of 150 °C was selected.

In parallel, the vulcanization degree was analyzed after 30 min at 150 °C using the moving die rheometer and vulcanization degrees of 68%, 77%, and 97% for respectively DCP2, DCP8, and S1 were obtained (Fig. S4). For the substrates vulcanized in the heated chamber during 30 min, based on hardness measurements, slightly lower vulcanization degrees of 58% for DCP2, 73% for DCP8 and 83% for S1 were reached. Thus, in spite of the absence of pressure in the heated chamber, vulcanization will occur simultaneously with spreading of the thermoplastic melt during contact angle measurements. Then, contact angle measurements were executed at 150 °C with PE melts on vulcanized and unvulcanized substrates of DCP2, DCP8 and S1.

Fig. 2 shows melting and spreading of a PE granule on vulcanized and unvulcanized DCP2 (a) and DCP8 (b). In Fig. 3, melting and spreading of PE on vulcanized and unvulcanized S1 is represented. The corresponding contact angles are represented in Fig. 4. After 3 min, a PE droplet was created and contact angles could be calculated. The initially unvulcanized substrates DCP2, DCP8 and S1 tended to increase in thickness (respectively with 23%, 7% and 11%) during vulcanization. This increase in thickness did not restrict the spreading process on the peroxide-based substrates DCP2 and DCP8 or on the sulfur-based substrate S1 as can be seen in Fig. 2 and Fig. 3 when comparing the droplet at 1 min with the droplet at 5 min which corresponds to a decrease in contact angles as shown in Fig. 4. When comparing images in Fig. 2 and the spreading dynamics in Fig. 4, a clear difference can be seen between vulcanized and unvulcanized peroxide-based EPDM substrates. While a significant contact angle relaxation process occurs on vulcanized DCP2 and DCP8, spreading on the unvulcanized substrates is restricted. Here, spreading is not dominated anymore by a physical process but by chemical bonding, in particular the formation of C—C bonds between EPDM and PE. Such bonds tend to retain the shape of the PE droplet as they originate from a co-vulcanization reaction caused by combination of allyl or alkyl EPDM radicals with alkyl PE radicals, or from addition of EPDM with alkyl PE radicals [25]. Contact angles on unvulcanized DCP2 do not significantly change anymore after 11 min (111.6° ± 4.3 at $t = 30$ min) because enough C—C bonds were formed preventing further spreading. In contrast, on vulcanized DCP2 contact angles continuously decrease in time (71.9° ± 1.7 at t = 30 min). Furthermore, on unvulcanized DCP8, PE is retained even more (129.7° ± 6.1 at t = 30 min) with a stabilization after 6 min, while spreading on vulcanized DCP8 is similar to DCP2, evidencing that adding 2 or 8 phr DCP does not change compatibility with PE [25]. The limitation in spreading on unvulcanized DCP substrates cannot be attributed to a polarity increase at the surface as no increase in chemical functional groups at the surface were found when comparing ATR-FTIR spectra of unvulcanized with vulcanized DCP (Fig. S5).

The reactive wetting results with a retained PE melt contradict findings by Grundke et al. [1], where an interfacial chemical reaction between the amino groups of poly(aminosiloxane) and the copolymer's maleic anhydride groups improved wetting at 130 °C. It is surmised that the spreading of the PE melt in the current study is restricted due to the uniqueness of the material combination as the PE chains at the interface become part of the three-dimensional rubber network during vulcanization [29]. The findings from this reactive wetting study were confirmed by the adhesion strength between EPDM and PE. Between DCP2 and PE an adhesion strength of 2.01 ± 0.08 MPa was reached. DCP8 with PE even lead to 4.28 ± 0.20 MPa [25]. Comparing these adhesion strengths to the total strength of each rubber (4.47 ± 0.12 MPa for DCP2; 7.49 ± 0.14 MPa for DCP8) shows an adhesion percentage of 45% for DCP 2 and 57% for DCP8 [25]. Thus, it can be concluded that a higher contact angle during reactive wetting corresponds to more chemical bonding which leads to a higher adhesion percentage as well.

To confirm that the differences between vulcanized and unvulcanized peroxide-based EPDM can be attributed to chemical bonding, measurements were also executed on sulfur-based EPDM substrates (S1). Interestingly, Figs. 3 and 4 show that good wetting occurs on both unvulcanized and vulcanized S1, with contact angles after 30 min that do not differ significantly (respectively 61.1° ± 4.9 and 56.2° ± 5.8 at $t = 30$ min). As expected, co-vulcanization between sulfur-curing EPDM and PE is impossible due to the absence of unsaturations in PE, and thus spreading of PE is related to a physical process. The difference in roughness Ra between vulcanized and initially unvulcanized S1 also does not seem to affect spreading as contact angles are not significantly different. Furthermore, Chen et al. [30] proposed a deformation of a soft

substrate due to formation of a wetting ridge at the contact line, limiting spreading. However, Shore A hardness of unvulcanized S1 was lowest (DCP2: 17.5 Sh A; DCP8: 21.7 Sh A; S1: 14.9 Sh A) making it the softest substrates, and here no limitation in spreading was observed. Thus, wetting measurements were not affected by ridge formation. The higher cure rate of S1 (Fig. S4) can also not be responsible for the different wetting behavior as the spreading of DCP8 was already restricted after 6 min which corresponds to a vulcanization degree of 25% according to Fig. S4. During the initial phase of curing, i.e. 0 to 30%, S1 does not show a faster cure rate than DCP2 and DCP8.

4. Conclusion

In summary, a high temperature contact angle measurement methodology is proposed to investigate chemical bonding between an EPDM rubber and PE. The testing temperature was selected to avoid formation of gas bubbles at the vulcanizing EPDM surfaces. This methodology was successful for identifying the adhesion mechanism of EPDM with PE. On vulcanizing EPDM, spreading of the PE melt was clearly restricted and high contact angles were obtained due to a co-vulcanization reaction at the interface. Furthermore, higher peroxide concentration caused a higher contact angle on vulcanizing EPDM, as more C—C bonds can be formed, which can be related to a higher adhesion strength as well [25]. In future studies, a further validation of the proposed methodology will be performed to verify the relation between practical work of adhesion, caused by chemical bonding, and the contact angle on unvulcanized peroxide-based EPDM. Furthermore, additional structural and morphological analysis will be executed to validate the adhesion mechanism at the EPDM-PE interface, e.g. SEM-EDS under low vacuum or VE-AFM.

Funding

Funding: This work was supported by Research Foundation – Flanders (FWO) [1SB0319N].

Declaration of Competing Interest

The authors declare that they have no known competing financial interests or personal relationships that could have appeared to influence the work reported in this paper.

Acknowledgments

B. Laing acknowledges Research Foundation – Flanders (FWO) for funding this PhD Fellowship strategic basic research (1SB0319N). The authors also acknowledge the company Hercorub NV, Belgium for mixing and providing the uncured rubber material.

Appendix A. Supplementary data

Supplementary data to this article can be found online at https://doi.org/10.1016/j.colcom.2020.100343.

References

[1] K. Grundke, S. Michel, K.J. Eichhorn, D. Beyerlein, T. Bayer, Influence of chemical interactions on the macroscopic spreading of a maleic anhydride copolymer melt, Macromol. Chem. Phys. 203 (2002) 937–946, https://doi.org/10.1002/1521-3935(20020401)203:7<937::AID-MACP937>3.0.CO;2-C.
[2] F. Awaja, M. Gilbert, G. Kelly, B. Fox, P.J. Pigram, Adhesion of polymers, Prog. Polym. Sci. 34 (2009) 948–968, https://doi.org/10.1016/j.progpolymsci.2009.04.007.
[3] E. Jabbari, N.A. Peppas, Polymer-polymer interdiffusion and adhesion, J. Macromol. Sci. Part C 34 (1994) 205–241, https://doi.org/10.1080/15321799408009635.
[4] G. Kumar, K.N. Prabhu, Review of non-reactive and reactive wetting of liquids on surfaces, Adv. Colloid Interf. Sci. 133 (2007) 61–89, https://doi.org/10.1016/j.cis.2007.04.009.
[5] D. Bonn, J. Eggers, J. Indekeu, J. Meunier, E. Rolley, Wetting and spreading 81, 2009, pp. 739–805, https://doi.org/10.1103/RevModPhys.81.739.
[6] G. Bracco, B. Holst, Surface science techniques, 2013, https://doi.org/10.1007/978-3-642-34243-1.
[7] M. Vuckovac, M. Latikka, K. Liu, T. Huhtamäki, R.H.A. Ras, Uncertainties in contact angle goniometry, Soft Matter 15 (2019) 7089–7096, https://doi.org/10.1039/c9sm01221d.
[8] C.W. Karl, M. Klüppel, Characterization of elastomers by wetting: roughness and chemical heterogeneity, Chem. List. 105 (2011) 7–9.
[9] C.W. Karl, W. Rahimi, A. Lang, U. Giese, M. Klüppel, H. Geisler, Review - characterization of modified elastomer surfaces by wetting, KGK Kautschuk Gummi Kunststoffe 71 (2018) 19–31.
[10] G. Zitzenbacher, Z. Huang, M. LÃ¤ngauer, C. Forsich, C. Holzer, Wetting behavior of polymer melts on coated and uncoated tool steel surfaces, J. Appl. Polym. Sci. 133 (2016) 1–10, https://doi.org/10.1002/app.43469.
[11] G.J. Bex, D. Seveno, J. De Keyzer, F. Desplentere, A. Van Bael, Wetting measurements as a tool to predict the thermoplastic/thermoset rubber compatibility in two-component injection molding, J. Appl. Polym. Sci. 135 (2017) 12–14, https://doi.org/10.1002/app.46046.
[12] Y. Zhang, C.A. Fuentes, R. Koekoekx, C. Clasen, A.W. Van Vuure, J. De Coninck, D. Seveno, Spreading dynamics of molten polymer drops on glass substrates, Langmuir. 33 (2017) 8447–8454, https://doi.org/10.1021/acs.langmuir.7b01500.
[13] C.A. Fuentes, Y. Zhang, H. Guo, W. Woigk, K. Masania, C. Dransfeld, C. Dupont-Gillain, J. De Coninck, D. Seveno, A.W. Van Vuure, Predicting the adhesion strength of thermoplastic/glass interfaces from wetting measurements, Coll. Surf. A Physicochem. Eng. Asp. 558 (2018) 280–290, https://doi.org/10.1016/j.colsurfa.2018.08.052.
[14] X. Zhang, B. Sun, N. Zhao, Q. Li, J. Hou, W. Feng, Experimental study on the surface characteristics of Pd-based bulk metallic glass, Appl. Surf. Sci. 321 (2014) 420–425, https://doi.org/10.1016/j.apsusc.2014.09.189.
[15] A. Marmur, Solid-surface characterization by wetting, Annu. Rev. Mater. Res. 39 (2009) 473–489, https://doi.org/10.1146/annurev.matsci.38.060407.132425.
[16] P.G. De Gennes, The dynamics of reactive wetting on solid surfaces 249, 1998, pp. 196–205.
[17] B. Komolafe, M. Medraj, Progress in Wettability Study of Reactive Systems 2014, 2014.
[18] L. Yin, B.T. Murray, S. Su, Y. Sun, Y. Efraim, H. Taitelbaum, T.J. Singler, Reactive wetting in metal – metal systems, 2009, https://doi.org/10.1088/0953-8984/21/46/464130.
[19] N. Eustathopoulos, R. Voytovych, The role of reactivity in wetting by liquid metals: a review, J. Mater. Sci. 51 (2016) 425–437, https://doi.org/10.1007/s10853-015-9331-3.
[20] K. Grundke, P. Uhlmann, T. Gietzelt, B. Redlich, Studies on the wetting behaviour of polymer melts on solid surfaces using the Wilhelmy balance method, 1996.
[21] G.J. Bex, F. Desplentere, J. De Keyzer, A. Van Bael, Two-component injection moulding of thermoset rubber in combination with thermoplastics by thermally separated mould cavities and rapid heat cycling, Int. J. Adv. Manuf. Technol. 92 (2017) 2599–2607, https://doi.org/10.1007/s00170-017-0341-y.
[22] W. Six, G. Bex, A. Van Bael, J. De Keyzer, F. Desplentere, Prediction of interfacial strength of HDPE overmolded with EPDM, Polym. Eng. Sci. 59 (2019) 1489–1498, https://doi.org/10.1002/pen.25148.
[23] G.-J. Bex, W. Six, B. Laing, J. De Keyzer, F. Desplentere, A. Van Bael, Effect of process parameters on the adhesion strength in two-component injection molding of thermoset rubbers and thermoplastics, J. Appl. Polym. Sci. 135 (2018), https://doi.org/10.1002/app.46495.
[24] B. Laing, J. De Keyzer, D. Seveno, A. Van Bael, Effect of co-agents on adhesion between peroxide cured ethylene–propylene–diene monomer and thermoplastics in two-component injection molding, J. Appl. Polym. Sci. 48414 (2019) 48414, https://doi.org/10.1002/app.48414.
[25] B. Laing, J. De Keyzer, D. Seveno, A. Van Bael, Adhesion between ethylene-propylene-diene monomer and thermoplastics in two-component injection molding: effect of dicumylperoxide as curing agent, J. Appl. Polym. Sci. (2020) 49233, https://doi.org/10.1002/app.49233.
[26] F. Awaja, P.J. Pigram, Surface molecular characterisation of different epoxy resin composites subjected to UV accelerated degradation using XPS and ToF-SIMS, Polym. Degrad. Stab. 94 (2009) 651–658, https://doi.org/10.1016/j.polymdegradstab. 2009.01.001.
[27] K. Bruckmoser, K. Resch, T. Kisslinger, T. Lucyshyn, Measurement of interdiffusion in polymeric materials by applying Raman spectroscopy, Polym. Test. 46 (2015) 122–133, https://doi.org/10.1016/j.polymertesting.2015.07.004.
[28] R. Orza, Investigation of Peroxide Crosslinking of EPDM Rubber by Solid-state NMR.Thesis, Eindhoven University of Technology, Eindhoven University of Technology, 2008, https://doi.org/10.6100/IR637815.
[29] J. Kruželák, R. Sýkora, I. Hudec, Vulcanization of rubber compounds with peroxide curing systems, Rubber Chem. Technol. 90 (2017) 60–88, https://doi.org/10.5254/rct.16.83758.
[30] L. Chen, E. Bonaccurso, T. Gambaryan-Roisman, V. Starov, N. Koursari, Y. Zhao, Static and dynamic wetting of soft substrates, Curr. Opin. Colloid Interface Sci. 36 (2018) 46–57, https://doi.org/10.1016/j.cocis.2017.12.001.